Resonance fluorescence from a three-level system

Chun-rong Fu
Department of Physics, Nanjing University, Nanjing, People's Republic of China

Yue-ming Zhang
Department of Physics, Nanjing Medical College, Nanjing, People's Republic of China

Chang-de Gong
Center of Theoretical Physics, Chinese Center of Advanced Science and Technology (World Laboratory), Beijing, People's Republic of China
and Department of Physics, Nanjing University, Nanjing, People's Republic of China
(Received 5 November 1990; revised manuscript received 24 April 1991)

The Green's-function method is used to study the properties of the spectrum of a three-level system driven by two resonant monochromatic fields. In the case of strong fields, we find that the correlation between two transitions is too small to consider. The Green's functions describing the two transitions consist of five Lorentzian lines rather than seven lines; furthermore, the positions at which sidebands are peaked depend on both Rabi frequencies, and only when two Rabi frequencies reach certain values can five Lorentzian lines appear. The heights of the sidebands become larger with increasing Rabi frequencies. The decay rates also affect the spectrum strongly.

PACS number(s): 32.80.−t, 32.50.+d, 42.50.−p

I. INTRODUCTION

In the past ten years, the quantum jumps in a three-level system have drawn considerable attention. There have been a number of discussions in the literature concerning the possibility of observing quantum jumps in atomic systems [1–5]. The systems currently under discussion involve the double-resonance scheme illustrated in Fig. 1.

In the V system, two excited states $|2\rangle$ and $|3\rangle$ are connected to a common lower level $|1\rangle$ via a strong and weak transition, respectively. Fluorescence photons from the strong transition are observed. However, an excitation of the weak transition where the electron is temporarily stuck in the metastable level $|2\rangle$ will cause the strong transition to be turned off. It is, therefore, possible to monitor the quantum jumps of the weak transition via the microscopic signal provided by the fluorescence of the strong transition. In the language of quantum measurement theory [6], the fluorescence from the strong transition acts as a pointer from which the microscopic quantum state of the atom may be determined. A similar effect may be observed for an atom in the Λ and L configurations shown in Figs. 1(b) and 1(c).

Since the weak-transition linewidth may be exceptionally narrow, the effect just described is of great interest, and has a wide application in both experiment and theory [7].

In this paper, we concentrate on the resonance fluorescence spectrum and its related behaviors. A more accurate calculation is made using Green's functions. Some results are then obtained to compare with the conclusion drawn by the former authors. In Sec. II, the Hamiltonian for V system is considered and discussed; this Hamil-

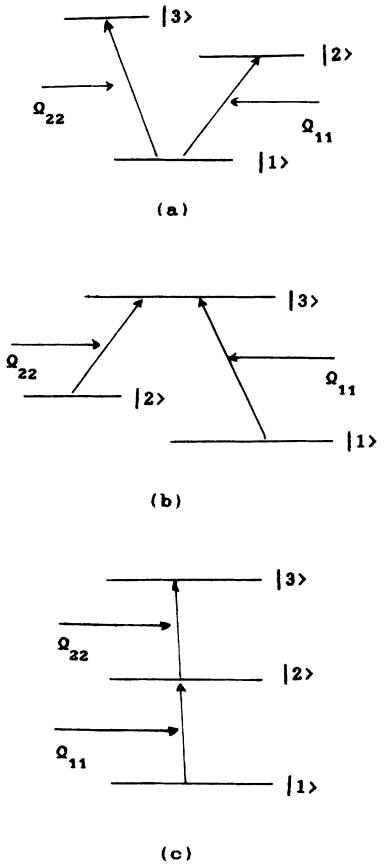

FIG. 1. Schematic diagrams of three-level systems driven by two laser fields. (a) V system. (b) Λ system. (c) L system.

tonian is then used to derive the double-time Green's functions which describe two transitions $1\rightarrow 2$ and $1\rightarrow 3$. In Sec. III, according to the conclusion in Sec. II, Λ and L systems will be investigated. We calculate all numerical results in Sec. IV. In Sec. V, some concluding remarks are given.

II. FORMULATION FOR V SYSTEM

We consider resonance fluorescence from a three-level system in a V configuration as shown in Fig. 1(a) where the energy levels for the ground state and the two excited states are denoted by $|1\rangle, |2\rangle$, and $|3\rangle$ and the corresponding energies by Ω_1, Ω_2 and Ω_3, respectively, with $\Omega_1<\Omega_2<\Omega_3$. The atom is resonantly driven by two laser fields whose energy modes ω_1 and ω_2 are initially populated and the electromagnetic field, these being initially unpopulated. The we write the Hamiltonian for such a system as [8,9]

$$H=H_0+H_r+H_{ir} , \tag{1}$$

$$H_0=\sum_{i=1}^{3}\Omega_i R_{ii}+\omega_1 b_1^{\dagger}b_1+\omega_2 b_2^{\dagger}b_2 + ig_1(b_1^{\dagger}R_{12}-b_1R_{21})+ig_2(b_2^{\dagger}R_{13}-b_2^{\dagger}R_{31}) , \tag{2}$$

$$H_r=\sum_{k,\lambda}ck\beta_{k\lambda}^{\dagger}\beta_{k\lambda} , \tag{3}$$

$$H_{ir}=\sum_{k,\lambda}ig_1(k)(R_{12}\beta_{k\lambda}^{\dagger}-\beta_{k\lambda}R_{21}) + \sum_{k,\lambda}ig_2(k)(R_{12}\beta_{k\lambda}^{\dagger}-\beta_{k\lambda}R_{31}) , \tag{4}$$

where the projective operators $R_{mm}=|m\rangle\langle n|$ obey the usual commutation relations

$$[R_{mn},R_{pq}]=R_{mq}\delta_{np}-R_{pn}\delta_{qm} \tag{5}$$

and the closure property

$$R_{11}+R_{22}+R_{33}=1 \tag{6}$$

while $b_1^{\dagger},b_2^{\dagger}$, and b_1,b_2 are the photon creation and annihilation operators for the pump fields and satisfy Bose statistics. The photon creation and annihilation operators $\beta_{k\lambda}$ and $\beta_{k\lambda}$ describe the frequency modes of the electromagnetic field with wave vector $\mathbf{k}$, frequency ck, and transverse polarization $\lambda(1,2)$. Units with $\hbar=1$ are used throughout.

The terms in Eq. (2) describe the free atomic and pump fields and the resonant interactions between them. Equations (3) and (4) represent the free electromagnetic field and its interaction with the electronic states 1, 2, and, 3 respectively. The driven fields are assumed to be strong while the photon field may be taken as the weakest of the three. Thus in our calculation, the high-order terms of Green's functions relevant to the photon field will be ignored.

We shall make use of the Fourier transform of the retarded double-time Green's function defined by [9]

$$G_{12}^{v}(\omega)=\langle\langle R_{12},R_{21}\rangle\rangle , \tag{7}$$

$$G_{13}^{v}(\omega)=\langle\langle R_{13},R_{31}\rangle\rangle . \tag{8}$$

$G_{12}^{v}(\omega)$ and $G_{13}^{v}(\omega)$ describe the transition $1\rightarrow 2$ and $1\rightarrow 3$, respectively.

Using Eqs. (2)–(4) and (7), we derive the following equations of motion:

$$(\omega-\omega_1-\tfrac{1}{2}\gamma_1)G_{12}^{v}(\omega)=\langle 2R_{12}^{z}\rangle-2ig_1\langle\langle R_{12}^{z}b_1,R_{21}\rangle\rangle +ig_2\langle\langle R_{32}b_2,R_{21}\rangle\rangle +\tfrac{1}{2}\gamma_{12}\langle\langle R_{13},R_{21}\rangle\rangle , \tag{9}$$

$$(\omega-\omega_2-\tfrac{1}{2}\gamma_2)\langle\langle R_{13},R_{21}\rangle\rangle=-2ig_2\langle\langle R_{13}^{z}b_2,R_{21}\rangle\rangle +ig_1\langle\langle R_{23}b_1,R_{21}\rangle\rangle +\tfrac{1}{2}\gamma_{12}G_{12}^{v}(\omega) , \tag{10}$$

where

$$\gamma_1=2\sum_{k,\lambda}\frac{g_i^2(k)}{\omega-ck},\quad \gamma_{12}=2\sum_{k,\lambda}\frac{g_1(k)g_2(k)}{\omega-ck} , \tag{11}$$

$$R_{mn}^{z}=\tfrac{1}{2}(|m\rangle\langle m|-|n\rangle\langle n|) . \tag{12}$$

Equations (9) and (10) tell us that the transition $1\rightarrow 3$ can take effect on transition $1\rightarrow 2$ by the coupling coefficient γ_{12}.

Although we have assumed that the transition $2\rightarrow 3$ is forbidden, the function γ_{12} gives the indirect coupling between the states 2 and 3 through the ground level 1. In fact, this coupling effect is so little that it can be ignored without influence on the results. If the separation between levels 2 and 3 is large, i.e., $|(\omega_1-\omega_2)/\gamma_1|\gg 1$, by calculating the numerical results, we can prove that γ_{12} has no effects on the spectrum. In order to obtain the expression for $G_{12}^{v}(\omega)$, we need to derive all of the equations of motion, which consists of 14 equations. These equations form a closed set of equations for $G_{12}^{v}(\omega)$. Of all of the equations, seven equations express the contribution from the transition $1\rightarrow 3$. We shall not write out all of the equations of motion in order to make the paper terse and only give the numerical results for the case in which all equations are considered. If we neglect the terms which contain γ_{12}, then the equations may be simplified greatly, in this case, we get

$$(\omega-\omega_1-\tfrac{1}{2}\gamma_1)G_{12}^{v}(\omega)=\langle 2R_{12}^{z}\rangle\left[1+\frac{A_2}{1-2A_2}\right] , \tag{13}$$

where

$$A_2=\frac{(1+0.5A_1)\Omega_{11}^2/2}{[\omega-\omega_1-\gamma_1(1+0.5A_1)](\omega-\omega_1-0.5\gamma_1)} +\frac{\Omega_{22}^2/4}{(\omega-\omega_1-0.5\gamma_1)(\omega-\omega_1-0.5\gamma_2)} , \tag{14}$$

$$A_1=\frac{\frac{1}{2}\gamma_2+(\Omega_{22}^2/2)/(\omega-\omega_1-0.50\gamma_2)}{\omega-\omega_1-\gamma_2-\Omega_{22}^2/(\omega-\omega_1-0.5\gamma_2)} , \tag{15}$$

$\Omega_{11}=2g_1\sqrt{\bar{n}_1}$ and $\Omega_{22}=2g_2\sqrt{\bar{n}_2}$ are Rabi frequen-

cies, $\bar{n}_1=\langle b_1^\dagger b_1\rangle$ and $\bar{n}_2=\langle b_2^\dagger b_2\rangle$ are mean photons for two pump fields, respectively.

In the derivation process of equations of motion, we have made use of the decoupling approximation such as

$$\langle\langle R_{13}^z b_2^\dagger b_2 b_1, R_{21}\rangle\rangle = 2\bar{n}_2\langle\langle R_{13}^z b_1, R_{21}\rangle\rangle \ . \tag{16}$$

The Green's function $G_{12}(\omega)$ given by Eq. (13) describes the spectrum of the transition $1\rightarrow 2$ with frequency ω_1. From Eq. (13) we find that there are one central peak at $\omega=\omega_1$ and two pairs of sidebands with the frequencies near $\omega_1\pm\Omega_{11}$ and $\omega_1\pm\Omega_{22}$.

The effect of interference between two pump fields is included in the frequency shifts, so that the two sidebands do not peak at the frequencies $\omega_1\pm\Omega_{11}$ and $\omega_1\pm\Omega_{22}$ exactly. It should be noted that the system considered here has no seven Lorentzian lines as mentioned by [10]. The results will be discussed in detail in Secs. III and IV.

By using the same method of deriving $G_{12}^v(\omega)$, we get the following expression for $G_{13}^v(\omega)$:

$$G_{13}^v(\omega)=\frac{\langle 2R_{13}^z\rangle}{\omega-\omega_2-0.5\gamma_2}\left[1+\frac{B_2}{1-2B_2}\right] , \tag{17}$$

$$B_2=\frac{(1+0.5B_1)\Omega_{22}^2/2}{[\omega-\omega_2-\gamma_2(1+0.5B_1)](\omega-\omega_2-0.5\gamma_2)} + \frac{\Omega_{11}^2/4}{(\omega-\omega_2-0.5\gamma_2)(\omega-\omega_2-0.5\gamma_1)} , \tag{18}$$

$$B_1=\frac{\frac{1}{2}\gamma_1+(\Omega_{11}^2/2)/(\omega-\omega_2-0.5\gamma_1)}{\omega-\omega_2-\gamma_1-\Omega_{11}^2/(\omega-\omega_2-0.5\gamma_1)} . \tag{19}$$

The Green's function $G_{13}^v(\omega)$ described by Eq. (17) represents the transition $1\rightarrow 3$. The spectrum structure is the same as that described by $G_{12}(\omega)$.

As a special case, placing $\Omega_{22}=0$ in Eq. (13) or $\Omega_{11}=0$ in Eq. (17), we can get the results which are identical to that of Ref. [9] and describe the excitation spectrum of a two-level atom driven by a strong pump field. Expressions (13) and (17) for the Green's functions $G_{12}^v(\omega)$ and $G_{13}^v(\omega)$ will be used to calculate numerically the excitation spectrum of the system under consideration.

III. Λ AND L SYSTEMS

As shown in Fig. 1(b), Λ and L systems are different from the V system. For example, the Λ system has a common high level, and the decay rate γ_3 does not vanish, which is added phenomenologically to obtain the nonvanishing steady-state resonance spectrum. We can, for the simplification, write the Hamiltonian for Λ and L systems together as follows:

$$\hat{H}=\hat{H}_0+\hat{H}_{ir} , \tag{20}$$

$$\hat{H}=\begin{bmatrix}H^\Lambda\\ H^L\end{bmatrix},\quad \hat{H}_0=\begin{bmatrix}H_0^\Lambda\\ H_0^L\end{bmatrix},\quad \hat{H}_{ir}=\begin{bmatrix}H_{ir}^\Lambda\\ H_{ir}^L\end{bmatrix},\quad \hat{1}=\begin{bmatrix}1\\ 1\end{bmatrix} , \tag{21}$$

where the upper indices Λ and L refer to Λ and L systems, respectively. The detailed expression of each term in (41) is given as follows [10,11]:

$$\hat{H}_0=\sum_{i=1}^{3}\Omega_i R_{ii}\hat{1}+\hat{\omega}_1 b_1^\dagger b_1+\hat{\omega}_2 b_2^\dagger b_2 + ig_1(b_1^\dagger\hat{R}_1-b_1\hat{R}_1^*)+ig_2(b_2^\dagger R_{23}+b_2 R_{32})\hat{1} , \tag{22}$$

$$\hat{H}_{ir}=\sum_{k,\lambda}[ig_1(k)(\hat{R}_1\beta_{k\lambda}^\dagger-\beta_{k\lambda}\hat{R}_1^*) + ig_2(k)(R_{23}\beta_{k\lambda}{}^\dagger-\beta_{k\lambda}R_{32}) + ig_3(k)(\hat{R}_3\beta_{k\lambda}^\dagger-\beta_{k\lambda}R_3^*)]+\sum_{k,\lambda}ck\beta_{k\lambda}^\dagger\beta_{k\lambda} , \tag{23}$$

$$\hat{\omega}_i=\begin{bmatrix}\omega_i^\Lambda\\ \omega_i^L\end{bmatrix},\quad \hat{R}_1=\begin{bmatrix}R_{13}\\ R_{12}\end{bmatrix},\quad \hat{R}_3=\begin{bmatrix}R_{12}\\ 0\end{bmatrix} ,$$

$$\omega_1^\Lambda=\Omega_3-\Omega_1,\quad \omega_2^\Lambda=\Omega_3-\Omega_2 ,$$

$$\omega_1^L=\Omega_2-\Omega_1,\quad \omega_2^L=\Omega_3-\Omega_2 .$$

The physical meaning of each term in Eqs. (22) and (23) is similar to that in Eq. (1). We define the Fourier transform of the retarded Green's function as

$$G_{13}^\Lambda(\omega)=\langle\langle R_{13},R_{13}\rangle\rangle,\quad G_{23}^\Lambda(\omega)=\langle\langle R_{23},R_{32}\rangle\rangle , \tag{24}$$

$$G_{12}^L(\omega)=\langle\langle R_{12},R_{21}\rangle\rangle,\quad G_{23}^L(\omega)=\langle\langle R_{23},R_{32}\rangle\rangle . \tag{25}$$

Let us, at first, discuss the L system. Making use of the same procedure and same decoupling approximation as we did previously, we get all equations of motion for $G_{12}^L(\omega)$ as follows:

$$(\omega-\omega_1-0.5\gamma_1)G_{12}^L(\omega)=\langle 2R_{12}^z\rangle-2ig_1\langle\langle R_{12}^Z b_1,R_{21}\rangle\rangle + ig_2\langle\langle R_{13}b_2^\dagger,R_{21}\rangle\rangle , \tag{26}$$

$$(\omega-\omega_1-\gamma_1)\langle\langle R_{12}^z b_1,R_{21}\rangle\rangle = ig_1\langle\langle R_{12}b_1^\dagger b_1,R_{21}\rangle\rangle - 0.5g_2\langle\langle R_{23}b_2^\dagger b_1,R_{21}\rangle\rangle - 0.5\gamma_2\langle\langle R_{23}^Z b_1,R_{21}\rangle\rangle , \tag{27}$$

$$(\omega-\omega_1-0.5\gamma_2)\langle\langle R_{13}b_2^\dagger R_{21}\rangle\rangle = ig_1\langle\langle R_{23}b_2^\dagger b_1,R_{21}\rangle\rangle - ig_2\langle\langle R_{12}b_2{}^+ b_2,R_{21}\rangle\rangle , \tag{28}$$

$$\left[\omega-\omega_1-\frac{\gamma_1+\gamma_2}{2}\right]\langle\langle R_{23}b_2^\dagger b_1,R_{21}\rangle\rangle = -2ig_1\bar{n}_1\langle\langle R_{13}b_2^\dagger,R_{21}\rangle\rangle-4ig_2\bar{n}_2\langle\langle R_{23}^Z b_1,R_{21}\rangle\rangle , \tag{29}$$

$$(\omega-\omega_1-\gamma_2)\langle\langle R_{23}^z b_1,R_{21}\rangle\rangle = -0.5ig_1\langle\langle R_{12}b_1^\dagger b_1,R_{21}\rangle\rangle + ig_2\langle\langle R_{23}b_2^\dagger b_1,R_{21}\rangle\rangle - 0.5\gamma_1\langle\langle R_{12}^z b_1,R_{21}\rangle\rangle , \tag{30}$$

$$(\omega-\omega_1-0.5\gamma_1)\langle\langle R_{12}b_1^\dagger b_1,R_{21}\rangle\rangle = \langle 2R_{12}^z\rangle\bar{n}_1-4ig_1\bar{n}_1\langle\langle R_{12}^z b_1,R_{21}\rangle\rangle, +2ig_2\bar{n}_1\langle\langle R_{13}b_2^\dagger,R_{21}\rangle\rangle , \tag{31}$$

$$(\omega-\omega_1-0.5\gamma_1)\langle\langle R_{12}b_2^\dagger b_2,R_{21}\rangle\rangle = \langle 2R_{12}^z\rangle\bar{n}_2-4ig_1\bar{n}_2\langle\langle R_{12}^z b_1,R_{21}\rangle\rangle +2ig_2\bar{n}_2\langle\langle R_{13}b_2^\dagger,R_{21}\rangle\rangle . \tag{32}$$

In deriving the equations the indirect coupling function γ_{12} has been neglected due to the same reasons as stated previously.

It is easy to find that Eqs. (26) and (31) are the same as Eqs. (28b) and (31) in Ref. [10], but the rest of the equations are different. This is because a rough approximation was used to calculate the equations of motion for $\langle\langle R_{12}^z b_1,R_{21}\rangle\rangle$, $\langle\langle R_{13}b_2^\dagger,R_{21}\rangle\rangle$, and $\langle\langle R_{23}b_2^\dagger b_1,R_{21}\rangle\rangle$ in that literature, furthermore, many terms were ignored in simplifying the Green's function to obtain the spectrum expression. As a result, the conclusion that seven Lorentzian lines appear in this case may not be the truth. If we neglect the last terms in Eqs. (27) and (29), the same result in Ref. [10] will be obtained. It is clear that our results are more exact than that of reference [10].

Thus in the case of double resonance, the three-level system only has five Lorentzian lines. We will give the detailed results in next section.

Solving Eqs. (26)–(32), we get

$$G_{12}^L(\omega)=\frac{\langle 2R_{12}^z\rangle}{\omega-\omega_1-0.5\gamma_1}\left[1+\frac{f_6}{1-2f_6}\right], \tag{33}$$

$$f_6=\frac{\frac{1}{2}\Omega_{11}^2 f_4+\frac{1}{4}\Omega_{22}^2 f_5}{f_3(\omega-\omega_1-0.5\gamma_1)}, \tag{34}$$

$$f_5=\frac{\frac{1}{2}\Omega_{11}^2[\omega-\omega_1-\gamma_1+0.5\gamma_1 f_1+(1-0.5f_1)\gamma_1]}{[\omega-\omega_1-(\gamma_1+\gamma_2)/2]\{\omega-\omega_1-\gamma_2-\Omega_{22}^2/[\omega-\omega_1-0.5(\gamma_1+\gamma_2)]\}+\omega-\omega_1-\gamma_1+0.5\gamma_1 f_1}, \tag{35}$$

$$f_4=(1-0.5f_1)f_2+\frac{\frac{1}{4}\Omega_{22}^2(1-2f_1)}{\omega-\omega_1-0.5(\gamma_1+\gamma_2)}\left[1+\frac{\frac{1}{2}\Omega_{11}^2}{[\omega-\omega_1-(\gamma_1+\gamma_2)/2]\{\omega-\omega_1-\gamma_2-\Omega_{22}^2/[\omega-\omega_1-0.5(\gamma_1+\gamma_2)]\}}\right], \tag{36}$$

$$f_3=(\omega-\omega_1-\gamma_1+0.5\gamma_1 f_1)f_2-\frac{\frac{1}{2}\gamma_1\Omega_{11}^2\Omega_{22}^2(1-0.5f_1)}{[\omega-\omega_1-(\gamma_1+\gamma_2)/2]^2\{\omega-\omega_1-\gamma_2-\Omega_{22}^2/[\omega-\omega_1-0.5(\gamma_1+\gamma_2)]\}}, \tag{37}$$

$$f_2=\omega-\omega_1-0.5\gamma_2-\frac{\frac{1}{2}\Omega_{11}^2}{\omega-\omega_1-0.5(\gamma_1+\gamma_2)}-\frac{\frac{1}{2}\Omega_{11}^2\Omega_{22}^2}{[\omega-\omega_1-(\gamma_1+\gamma_2)/2]^2\{\omega-\omega_1-\gamma_2-\Omega_{22}^2/[\omega-\omega_1-0.5(\gamma_1+\gamma_2)]\}}, \tag{38}$$

$$f_1=\frac{\frac{\gamma_2}{2}+\frac{1}{2}\Omega_{22}^2/[\omega-\omega_1-0.5(\gamma_1+\gamma_2)]}{\omega-\omega_1-\gamma_2-\Omega_{22}^2/[\omega-\omega_1-0.5(\gamma_1+\gamma_2)]} . \tag{39}$$

In the absence of the driven field 2, that is in the case in which $\Omega_{22}=0$ and $\gamma_2=0$, Eq. (33) becomes

$$G_{12}^L(\omega)=\frac{\langle R_{12}^z\rangle}{\omega-\omega_1-0.5\gamma_1}\left[1+\frac{\frac{1}{2}\Omega_{11}^2}{(\omega-\omega_1-0.5\gamma_1)(\omega-\omega_1-\gamma_1)-\Omega_{11}^2}\right]$$

which is identical to Eq. (36) in Ref. [9].

Using the similar approximation, we obtain the expression for $G_{23}^L(\omega)$ as follows:

$$G_{23}^L(\omega)=\frac{\langle 2R_{23}^z\rangle}{\omega-\omega_2-0.5\gamma_2}\left[1+\frac{h_6}{1-2h_6}\right], \tag{40}$$

$$h_6=\frac{\frac{1}{2}\Omega_{22}^2 h_4+\frac{1}{4}\Omega_{11}^2 h_5}{h_3(\omega-\omega_2-0.5\gamma_2)}, \tag{41}$$

$$h_5=(\omega-\omega_2-\gamma_2+0.5h_1\gamma_2)\times\left[1+\frac{\frac{1}{2}\Omega_{22}^2}{(\omega-\omega_2-0.5\gamma_1)h_0}\right] +\frac{\frac{1}{2}\gamma_2\Omega_{22}^2(1-0.5h_1)}{(\omega-\omega_2-0.5\gamma_1)h_0}, \tag{42}$$

$$h_4=(1-0.5h_1)h_2+\frac{\Omega_{11}^2(1-0.5h_1)}{\omega-\omega_2-0.5\gamma_1}\times\left[1+\frac{\frac{1}{2}\Omega_{22}^2}{(\omega-\omega_2-0.5\gamma_1)h_0}\right], \quad (43)$$

$$h_3=(\omega-\omega_2-\gamma_2+0.5\gamma_2h_1)h_0-\frac{\frac{1}{2}\Omega_{11}^2\Omega_{22}^2\gamma_2(1-0.5h_1)}{(\omega-\omega_2-0.5\gamma_1)^2h_0}, \quad (44)$$

$$h_2=\omega-\omega_2-0.5\gamma_2-\frac{\frac{1}{2}\Omega_{22}^2}{\omega-\omega_2-0.5\gamma_1}-\frac{\frac{1}{2}\Omega_{11}^2\Omega_{22}^2}{(\omega-\omega_2-0.5\gamma_1)^2h_0}, \quad (45)$$

$$h_1=-\frac{\frac{1}{2}\gamma_1+\frac{1}{2}\Omega_{11}^2/(\omega-\omega_2-0.5\gamma_1)}{h_0}, \quad (46)$$

$$h_0=\omega-\omega_2-\gamma_1-\frac{\Omega_{11}^2}{\omega-\omega_2-0.5\gamma_1}. \quad (47)$$

The expression (40) is similar to that of $G_{12}^L(\omega)$ given by Eq. (33).

For the Λ system, by making use of the same procedure in Sec. II, we can obtain the expressions for its Green's function

$$G_{13}^{\Lambda}(\omega)=\frac{\langle 2R_{13}^z\rangle}{\omega-\omega_1-0.5\gamma_1}\left[1+\frac{C_2}{1-2C_2}\right], \quad (48)$$

$$G_{23}^{\Lambda}(\omega)=\frac{(2R_{23}^z)}{\omega-\omega_2-0.5\gamma_2}\left[1+\frac{D_2}{1-2D_2}\right], \quad (49)$$

$$C_2=\frac{\frac{1}{2}\Omega_{11}^2(1+0.5C_1)/[\omega-\omega_1-\gamma_1(1+0.5C_1)]+\frac{1}{4}\Omega_{22}^2/(\omega-\omega_1-0.5\gamma_3)}{\omega-\omega_1-0.5\gamma_1}, \quad (50)$$

$$C_1=\frac{\frac{1}{2}\gamma_2+\frac{1}{2}\Omega_{22}^2/[\omega-\omega_1-0.5(\gamma_1+\gamma_2)]}{\omega-\omega_1-\gamma_2-\Omega_{22}^2/[\omega-\omega_1-0.5(\gamma_1+\gamma_2)]}, \quad (51)$$

$$D_2=\frac{\frac{1}{2}\Omega_{22}^2(1+0.5D_1)/[\omega-\omega_2-\gamma_2(1+0.5D_1)]+\frac{1}{4}\Omega_{11}^2/(\omega-\omega_2-0.5\gamma_3)}{\omega-\omega_2-0.5(\gamma_1+\gamma_2)}, \quad (52)$$

$$D_1=\frac{\frac{1}{2}\gamma_1+\frac{1}{2}\Omega_{11}^2/(\omega-\omega_2-0.5\gamma_1)}{\omega-\omega_2-\gamma_1-(\Omega_{11}^2/2)/(\omega-\omega_2-0.5\gamma_1)}. \quad (53)$$

It is clear that Eqs. (48) and (49) also give five Lorentzian lines, respectively.

IV. SPECTRUM FOR THE V SYSTEM

First of all, we make use of the Eqs. (9) and (10) and all equations concerning γ_{12} to prove that γ_{12} has no effect on the spectrum.

The expression (11) for γ_i has real and imaginary parts, the real parts, which give small energy shifts arising when principal values of the integrals are taken into account, will be neglected or they may be conveniently incorporated into the original definitions of ω_i while the imaginary parts are

$$\mathrm{Im}\gamma_1=\gamma_1^0=\frac{4}{3}\left[\frac{\omega_1}{c}\right]^3|P_{12}|^2, \quad (54)$$

$$\mathrm{Im}\gamma_2=\gamma_2^0=\frac{4}{3}\left[\frac{\omega_2}{c}\right]|P_{13}|^2. \quad (55)$$

With Eqs. (54) and (55), we obtain the numerical result as shown in Fig. 2. It is easy to find that the spectrum almost does not change with the increase of γ_{12}. This conclusion is valid by considering the relative order of magnitude for each term as follows:

The second and third terms in the right-hand side of Eq. (9) will be proportional to Ω_{11} and Ω_{22}, respectively, while γ_{12} only gives γ_0, normally we have $\Omega_{11}/\gamma_0>1, \Omega_{22}/\gamma_0>1$. In fact, the Green's functions contain the factors $(\Omega_{11}/\gamma_1)^2$ or $(\Omega_{22}/\gamma_1)^2$. Meanwhile, the transition $1\rightarrow3$ peaks at ω_2, usually $|\omega_2-\omega_1\gg\gamma_1^0$, denote, accordingly $(|\omega_2-\omega_1|/\gamma_1^0)(\Omega_{11}/\gamma_1^0)^2\gg1$. Thus the terms including γ_{12} have so little contribution to the spectrum that they can be ignored.

Now we may use Eqs. (13)–(15) and Eqs. (17)–(19) to compute the spectrum for the V system. The results are shown in Figs. 3(a) and 3(b). They describe the spectrum for $1\rightarrow2$ and $1\rightarrow3$ transitions, respectively. It is clear that each figure consists of five Lorentzian lines rather than seven Lorentzian lines. It seems that, according to stark effect, two pump fields should produce seven lines, however, since the pump field 1 is resonantly coupling

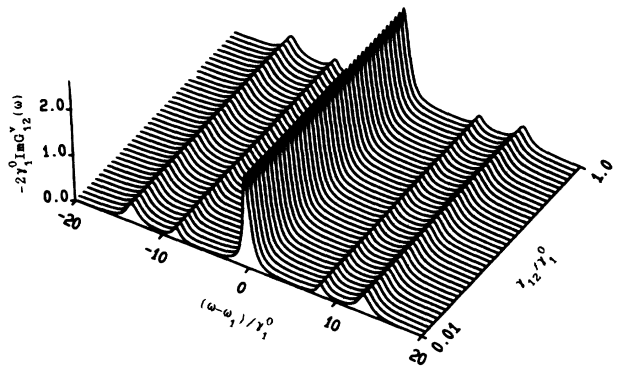

FIG. 2. Plot of resonance fluorescence spectrum for transition $1\rightarrow 2$ in the V system with the changes of γ_{12} $\Omega_{11}/\gamma_1^0=\Omega_{22}/\gamma_1^0=10.0$ $(\omega_2-\omega_1)/\gamma_1^0=10.0$.

with the transition $1\rightarrow 2$, the second field does not. The action of interference between two fields only affects the frequency shifts of the sidebands, and the second pump field cannot break the sidebands into two peaks. Figure 3(a) clearly illustrates this feature. Both the pair of inner sidebands and the pair of outer sidebands, with the increase of the Ω_{22}, which express the strength of the pump field, change the positions at which the lines peak. Furthermore it is not until Ω_{22} reaches certain value can all five Lorentzian lines appear, i.e., only when the second pump field is strong enough, could it excite the inner sidebands. We show this conclusion in Figs. 4(a) and 4(b). (a) is the critical values in which Ω_{11} and Ω_{22} are satisfied when all five Lorentzian lines appear. It should be noted that the relation between Ω_{11} and Ω_{22} is nonlinear, Ω_{22} increases in steplike shape when Ω_{11} changes. The height of each step is about equal to $0.5\gamma_1^0$—half spectral width. It is an interesting phenomenon. Our physical explanation is that the strength of the second pump field breaking the central peak is quantized; when the spectrum was first separated by the first driven field, the newly formed spectra would have been of a certain stability. The stronger the first field, the more difficult the second field separates the spectra.

When placing $\gamma_1^0=\gamma_2^0$, the spectral structure for transition $1\rightarrow 3$ is similar to that for transition $1\rightarrow 2$. It is necessary that we consider the effect of γ_2^0 on the spectrum. Figures 5(a) and 5(b) tell us that γ_2^0 has not remarkable influence on the central peak and the outer sidebands, but affects the inner sidebands strongly. When γ_2^0 decreases, the heights of the inner peaks become larger and the linewidth becomes narrower. These results state that the γ_2^0 and Ω_{22} play the leading role in producing the inner peaks in transition $1\rightarrow 2$. From Fig. 5(b) we see that the central peak grows higher and becomes narrower with the decrease of γ_2^0, while the sidebands have no changes. This preciously fine spectral line can provide an important measuring method.

It is clear that there are some differences between the results in Ref. [11] and ours. They stated that the areas

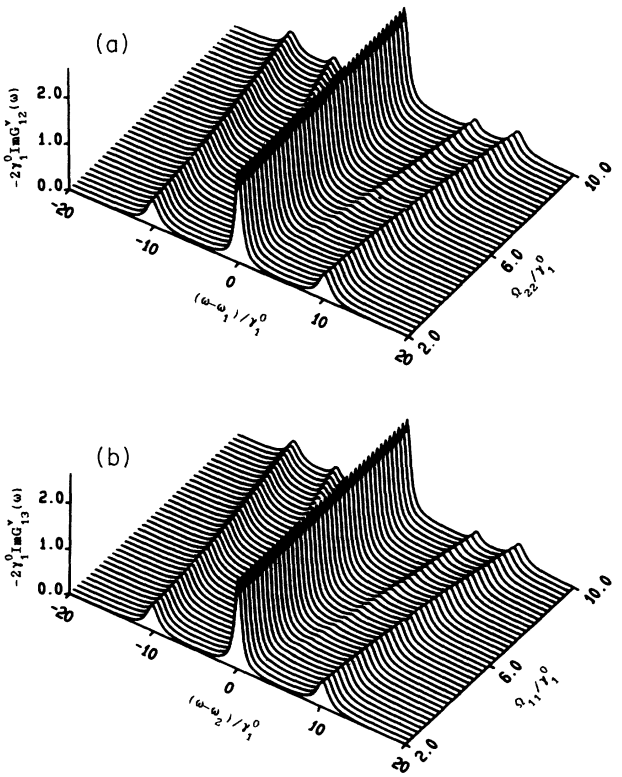

FIG. 3. Resonance fluorescence spectrum plots for the V system. (a) Transition $1\rightarrow 2$, $\Omega_{11}/\gamma_1^0=10.0$, $\gamma_2^0/\gamma_1^0=1.0$. (b) Transition $1\rightarrow 3$, $\Omega_{22}/\gamma_1^0=10.0$, $\gamma_2^0/\gamma_1^0=1.0$.

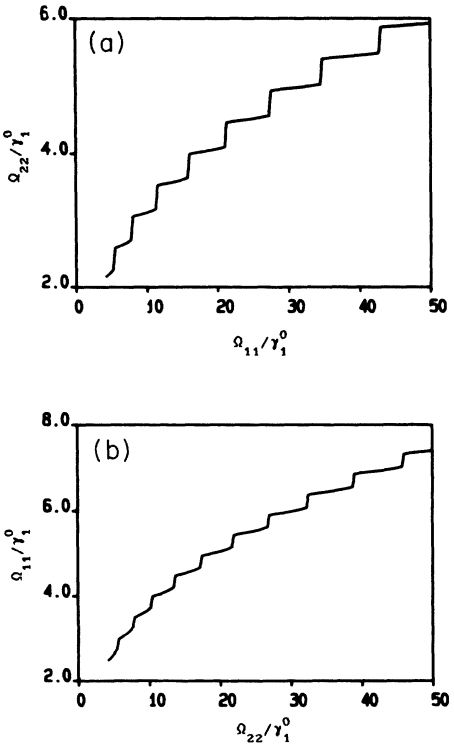

FIG. 4. Critical Rabi frequency plots for the appearance of five Lorentzian lines. $\gamma_2^0/\gamma_1^0=1.0$. (a) Transition $1\rightarrow 2$. (b) Transition $1\rightarrow 3$.

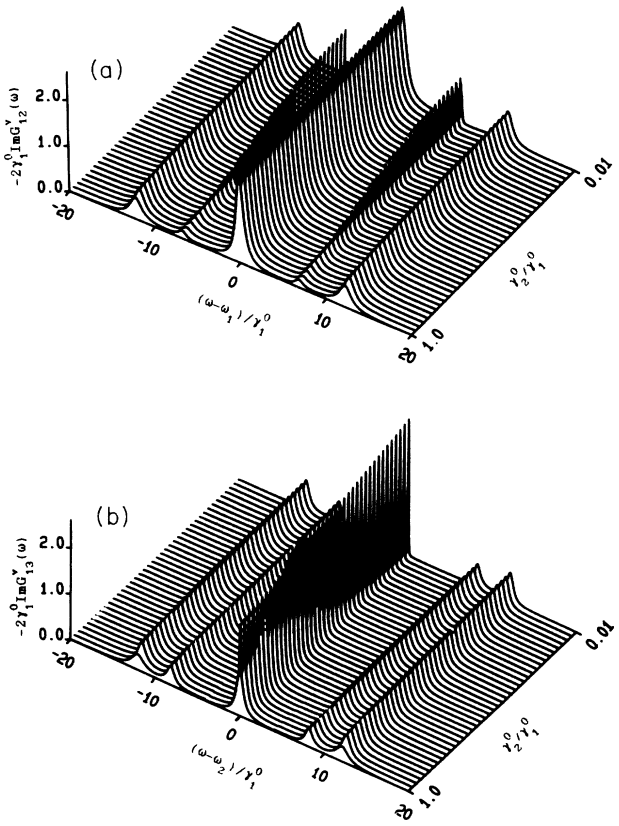

FIG. 5. The effect of γ_2 on the resonance fluorescence spectrum. (a) Transition $1\rightarrow 2$. $\Omega_{11}/\gamma_1^0=10.0$. $\Omega_{22}/\gamma_1^0=8.0$. (b) Transition $1\rightarrow 3$, $\Omega_{11}/\gamma_1^0=10.0$, $\Omega_{22}/\gamma_1^0=8.0$.

of the peaks in the lower-transition spectrum are in the ratio

$$|\Omega_{11}|^2/2:|\Omega_{22}|^2:|\Omega_{11}|^2:|\Omega_{22}|^2:|\Omega_{11}|^2/2 \ .$$

And for the upper transition the areas under the peaks are in the ratio

$$\gamma_2/2:\gamma_1:\gamma_2:\gamma_1:\gamma_2/2 \ .$$

On the other hand, the ratios in the lower transition depend only on the Rabi frequencies, while in the upper transition the ratios depend only upon the decay rates. We consider that these results may not be the truth. One can see that the decay rates determine the width of the spectrum and the Rabi frequencies affect the heights of the sidebands on both transitions, thus the decay rates and the Rabi frequencies play the same leading roles in the shape of the spectrum. It is impossible that only one factor decides the behavior of the spectrum. Figures 3(a), 3(b), 5(a), and 5(b) in our paper show clearly this fact.

The failure in Ref. [11] is due to the approximation of treating (3.4a)–(3.7b) in which the authors take the assumption that there is no correlation between the initial field operators and the atomic operators. In fact, the half Rabi frequency (the interaction energy in Ref. [11]) should be defined as

$$G_a^2=|g_a^\alpha|^2\langle C_\alpha^\dagger(0)C_\alpha((0))\rangle, \quad G_b^2=|g_b^\beta|^2\langle C_\beta^\dagger(0)C_\beta(0)\rangle \ .$$

Their definition resulted in the loss of some important correlating terms between two modes. That is, some second-order terms were neglected, while in our calculation, only those terms more than third-order were ignored; therefore, there are some differences between their results and ours.

Direct calculation shows that the Λ system and the L system also contain five components which are symmetric about the spectral center at the corresponding laser frequencies when the external laser fields are resonant and monochromatic. This is identical to Ref. [11], and the similar behaviors described previously in this paper are found in these two systems, too. Thus it is unnecessary to go into detail here. However, if we had used the same approximation in Ref. [10], we could also get the result that there are seven Lorentzian lines appearing. It proves that our conclusion is more precise.

V. SUMMARY

In this paper we have derived the Green's functions for three configurations. Under the assumption that the two driven fields are strongly resonant with the three-level atom, each system includes five Lorentzian lines which are symmetric about the central peak. If one of the fields is much weaker, the spectra only exhibit three peaks, which is characteristic of a strongly driven two-level atom. The critical Rabi frequencies satisfy an interesting relation. When the decay rate γ_2 is much smaller than γ_1, a very narrow spectral line can be produced. The Rabi frequency and γ_2 play an important role in the spectrum.

ACKNOWLEDGMENTS

This work is supported by the National Natural Science Foundation. The authors express their thanks to Dr. Xio-sheng Li for helpful discussions. C. D. Gong would like to thank Professor Abdus Salam, the International Atomic Energy Agency, and UNESCO for their hospitality during the author's stay at the International Centre for Theoretical Physics, Trieste, Italy.

[1] R. J. Cook and H. J. Kimble, Phys. Rev. Lett. **54**, 1023 (1985).
[2] A. Schenzle, R. G. Devoe, and R. G. Brewer, Phys. Rev. A **33**, 2127 (1986).
[3] J. Javanainen, Phys. Rev. A **33**, 2121 (1986).
[4] D. T. Pegg, R. Loudon, and P. L. Knight, Phys. Rev. A **33**, 4085 (1986).
[5] P. Zoller, M. Marle, and D. F. Walls, Phys. Rev. A **35**, 198 (1987).
[6] W. Zurek, Phys. Rev. D **24**, 1516 (1981); **26**, 1862 (1982).

[7] H. J. Kimble, R. J. Cook, and A. L. Walls, Phys. Rev. A **34**, 3190 (1986).
[8] N. N. Boglubov, Jr., F. L. Kien, and A. S. Shumovski, Phys. Lett. **101A**, 201 (1984).
[9] Chun-rong Fu and Chang-de Gong, Phys. Rev. A **40**, 207 (1989).
[10] C. Mavroyannis, Mol. Phys. **37**, 1175 (1979).
[11] R. M. Whitley and C. S. Stroud, Jr., Phys. Rev. A **14**, 1498 (1976).